Quantum Hall ferromagnets and transport properties of buckled Dirac materials

Wenchen Luo and Tapash Chakraborty
Department of Physics and Astronomy, University of Manitoba, Winnipeg, Canada R3T 2N2
(Received 23 June 2015; revised manuscript received 10 September 2015; published 14 October 2015)

We study the ground states and low-energy excitations of a generic Dirac material with spin-orbit coupling and a buckling structure in the presence of a magnetic field. The ground states can be classified into three types under different conditions: SU(2), easy-plane, and Ising quantum Hall ferromagnets. For the SU(2) and the easy-plane quantum Hall ferromagnets there are goldstone modes in the collective excitations, while all the modes are gapped in an Ising-type ground state. We compare the Ising quantum Hall ferromagnet with that of bilayer graphene and present the domain-wall solution at finite temperatures. We then specify the phase transitions and transport gaps in silicene in Landau levels 0 and 1. The phase diagram depends strongly on the magnetic field and the dielectric constant. We note that there exist triple points in the phase diagrams in Landau level $N = 1$ that could be observed in experiments.

DOI: 10.1103/PhysRevB.92.155123 PACS number(s): 73.43.−f

I. INTRODUCTION

Recently, several graphenelike systems, such as silicene, germanene [1], and transition-metal dichalcogenides (MoS_2) [2], have received considerable attention. They all have a honeycomb geometry in the xy plane as in graphene [3,4], but they also have a buckled structure in the z direction. The buckling is induced by the atoms that are heavier than the carbon atoms in graphene. The heavy atoms also have more complex electron orbitals. In these systems, spin-orbit (SO) coupling is important, while it is negligible in graphene. Hence, the electrons in these systems must be described by a massive Dirac equation in which the mass is induced by the SO coupling. We refer to these materials generically as buckled Dirac materials due to their geometric structure. The Brillouin zone is similar to that of graphene: a hexagon with two inequivalent valleys K and K'. In MoS_2, the Γ point is important because the energy near this point is close to that in the K, K' valleys in the valence band. For simplicity, we consider only the K and K' valleys in order to compare with graphene.

In the presence of a magnetic field, the electron bands split into a series of Landau levels (LLs). The fractional quantum Hall (QH) effect [5] has been studied recently in silicene and germanene [6]. The fractal butterflies have also been investigated theoretically in these systems [7]. Here we report on the ground states and transport properties of the symmetry broken states in the integer QH effect regime. In bilayer and multilayer graphene [9,10], earlier theoretical works have indicated that the ground states in the $N \neq 0$ LLs are Ising quantum Hall ferromagnets (QHFs), since the interlayer Coulomb potential is different from the intralayer one. The resulting transport properties of bilayer graphene were also observed in an experiment [11]. In buckled Dirac materials, the buckling divides the system into two "pseudolayers." Atoms A and B belong to different pseudolayers, respectively. Hence the buckling makes these monolayer Dirac materials similar to bilayer graphene, i.e., we could observe the Ising QHF in these one-atom-layer systems. We discuss below the classification and the collective modes of different QHFs in a few LLs.

The buckling also couples to an external electric field. Without the magnetic field, silicene and germanene may be converted to topological insulators in a proper electric field [12]. In the QH regime, the phases and transport properties are also much richer and more interesting when the electric field is applied. In this work, we will specifically discuss how the electric field and the dielectric constant (of different substrates) change the phase diagram and control the spin and valley pseudospin in silicene. These materials are potential candidates for application in (pseudo)spintronics.

II. NONINTERACTING HAMILTONIANS

We consider two actual materials, silicene and germanene, in a perpendicular electric field E_z. The electric field can control the phases and the spin polarization, useful for application in (pseudo)spintronics. The Brillouin zone is in general a regular hexagon (as in graphene) with two inequivalent valleys K and K'. The low-energy noninteracting Hamiltonian, in the basis $\{A\uparrow, B\uparrow, A\downarrow, B\downarrow\}$, is [13]

$$H_\eta = v_F(p_x\tau_x - \eta p_y\tau_y) + \eta\tau_z h + dE_z\tau_z/2, \qquad (1)$$

where $h = -\lambda_{SO}\sigma_z - a_0\lambda_R(p_y\sigma_x - p_x\sigma_y)$, $\eta = 1$ for valley K and -1 for the K' valley, τ and σ are the Pauli matrices corresponding to the sublattices and the spin, a_0 is the lattice constant, λ_R is the Rashba SO (RSO) coupling, and the buckling is d. For silicene [14,15], these parameters are $v_F = 5.5 \times 10^5$ m/s, $a_0 = 3.86$ Å, $\lambda_{SO} = 3.9$ meV, $\lambda_R = 0.7$ meV, and $d = 0.46$ Å. To classify the quantum Hall ferromagnets of the ground state analytically in a magnetic field, we approximate $\lambda_R = 0$ and set $E_z = 0$. At a quarter filling in a LL, the spin is polarized by the Zeeman coupling. Then the system is simplified to a two-level (two valleys) model. The Hamiltonian in one spin, which is similar to Haldane's model [16,17] or the Kane-Mele model [18] in one spin and may describe a generic monolayer Dirac material in this case, is

$$H_\eta = v_F(\tau_x P_x - \eta\tau_y P_y) - \lambda_{SO}\tau_z, \qquad (2)$$

where $\mathbf{P} = \mathbf{p} + e\mathbf{A}$ is the canonical momentum. The SO strength is also described as the mass of the Dirac fermion near each valley. We choose the Landau gauge of the vector potential $\mathbf{A} = (0, Bx, 0)$. The LL energy spectrum is given by

$E_0 = \pm\lambda_{\rm SO}$ and $E_{n\neq 0} = {\rm sgn}(n)\sqrt{\lambda_{\rm SO}^2 + 2(v_F\hbar/\ell)^2\sqrt{n^2+|n|}}$, where $\ell = \sqrt{\hbar/eB}$ is the magnetic length and n is the LL index. The eigen wave functions in the two valleys are [19]

$$\psi^K_{n,X} = \begin{pmatrix} \widetilde{a}h_{n,X} \\ \widetilde{b}h_{n-1,X} \end{pmatrix},\ \psi^{K'}_{n,X} = \begin{pmatrix} \widetilde{b}h_{n-1,X} \\ \widetilde{a}h_{n,X} \end{pmatrix}, \tag{3}$$

where X is the guiding center, and $h_{n,X}$ ($h_{n<0} = 0$) is the LL wave function of a two-dimensional electron gas (2DEG) in a conventional semiconductor. We define $a = |\widetilde{a}|, b = |\widetilde{b}|$, so the normalization condition is $a^2 + b^2 = 1$. In MoS_2, the Γ point should be included in the Hamiltonian. The low-energy effective Hamiltonian is due to the three d-orbitals of Mo atoms, which are located in the same plane [8]. So the MoS_2 is equivalent to a monolayer system without buckling.

III. CLASSIFICATION OF THE QUANTUM HALL FERROMAGNETIC GROUND STATES

If the geometry of the monolayer Dirac material is exactly the same as graphene, then the valley pseudospin has a SU(2) symmetry in any LL. However, we need to consider the buckling when we calculate the Coulomb interaction. The ground states of bilayer or chiral multilayer graphene in an $N \neq 0$ LL are valley pseudospin Ising QHFs [9,10]. The SU(2) symmetry of valley pseudospin is broken to a Z_2 symmetry because there is a factor e^{-qd} difference between the interlayer and intralayer Coulomb potentials, where q is the momentum and d is the distance between two layers. We follow the formalism in [9,10] to present a more general classification of the QHFs of the ground states in a buckled Dirac material. We assume a buckling d in the z direction between the two elements of the wave-function spinors in Eq. (3). The buckling divides the wave functions into two pseudolayers. The density matrix ρ in the momentum space is

$$\rho_{\sigma,\sigma'}(\mathbf{q}) = \frac{1}{N_\phi}\sum_{X_1,X_2} e^{-\frac{i}{2}q_x(X_1+X_2)}\delta_{X_1,X_2+q_y\ell^2}c^\dagger_{\sigma,X_1}c_{\sigma',X_2}, \tag{4}$$

where $\sigma,\sigma' = 1 \to (K,\uparrow), 2 \to (K,\downarrow), 3 \to (K',\uparrow), 4 \to (K',\downarrow)$ are the valley-spin indices, the LL degeneracy is N_ϕ, and the creation and annihilation operators of electrons are $c^\dagger, c$. The average values of the elements of the density matrix fully describe the system with the Hamiltonian in the Hartree-Fock approximation (HFA). The filling factor for level i is then given by $\nu_i = \langle\rho_{i,i}(0)\rangle$.

The many-body Hamiltonian in the Hartree-Fock approximation (HFA) is then given by

$$\begin{aligned} H = &\sum_\sigma E_\sigma\rho_{\sigma,\sigma}(0) + \frac{e^2}{\kappa\ell}\frac{d}{2\ell}\sum_{\sigma,\sigma'} y_{\sigma'}\langle\rho_{\sigma',\sigma'}(0)\rangle y_\sigma\rho_{\sigma,\sigma}(0) \\ &+ \frac{e^2}{\kappa\ell}\sum_{\sigma,\sigma'}\overline{\sum_{\mathbf{q}}} H_{\eta,\eta'}(\mathbf{q})\langle\rho_{\sigma,\sigma}(-\mathbf{q})\rangle\rho_{\sigma',\sigma'}(\mathbf{q}) \\ &- \frac{e^2}{\kappa\ell}\sum_{\sigma,\sigma'}\sum_{\mathbf{q}} X_{\eta,\eta'}(\mathbf{q})\langle\rho_{\sigma,\sigma'}(-\mathbf{q})\rangle\rho_{\sigma',\sigma}(\mathbf{q}), \end{aligned} \tag{5}$$

where κ is the dielectric constant, η and η' are the valley indices in σ and σ', respectively, and $y_1 = y_2 = a^2, y_3 = y_4 = -b^2$. E_σ is the kinetic energy of level σ with the Zeeman coupling. The summation with a bar excludes the term of $\mathbf{q} = \mathbf{0}$. The functions $H_{\eta,\eta'}$ and $X_{\eta,\eta'}$ describe the Hartree and Fock interactions between valleys η and η',

$$H_{\eta,\eta'}(\mathbf{q}) = \frac{1}{q\ell}\xi_{\eta,\eta'}(q\ell), \tag{6}$$

$$X_{\eta,\eta'}(\mathbf{q}) = \int_0^\infty dp\, J_0(pq\ell)\xi_{\eta,\eta'}(p), \tag{7}$$

where J is the Bessel function and

$$\xi_{\eta,\eta} = a^4 f_{n,n} + b^4 f_{n-1,n-1} + 2a^2b^2 f_{n,n-1}e^{-qd/\ell}, \tag{8}$$

$$\xi_{\eta,\overline{\eta}} = (a^4 f_{n,n} + b^4 f_{n-1,n-1})e^{-qd/\ell} + 2a^2b^2 f_{n,n-1}, \tag{9}$$

with $\overline{\eta}$ being the valley other than η. The function f is

$$f_{n,m}(q) = e^{-q^2/2}L_n(q^2/2)L_m(q^2/2), \tag{10}$$

with a Laguerre polynomial L_n ($L_{n<0} = 0$).

For a quarter filling of a LL, which is equivalent to the case of three-quarter filling due to the electron-hole symmetry, the ground state satisfies $\nu_1 + \nu_3 = 1$ and $\langle\rho_{1,3}(0)\rangle = \langle\rho_{3,1}(0)\rangle = \sqrt{\nu_1\nu_3}$, where we choose a property global phase to set all order parameters real. Hence, we obtain the energy per electron of the liquid phase by using the conditions $X_{K,K'} = X_{K',K}$, $X_{K,K} = X_{K',K'}$ and abandoning the constant kinetic energy,

$$E = 2\frac{e^2}{\kappa\ell}Q\nu_1(\nu_1 - 1), \tag{11}$$

where

$$\tilde{Q}(\mathbf{q}) = (a^2 - b^2)^2 d/\ell - X_{K,K}(\mathbf{q}) + X_{K,K'}(\mathbf{q}), \tag{12}$$

and $Q \equiv \tilde{Q}(\mathbf{q} = \mathbf{0})$. The first term in Eq. (12) is the capacitive energy. We can classify the ground states as follows. If $Q = 0$, the ground state is a SU(2) QHF, since ν_1 and ν_3 could be any value to minimize the energy. If $Q < 0$, the ground state is an Ising QHF. The energy is minimized when ν_1 is either 0 or 1. Finally, if $Q > 0$, the ground state is an easy-plane QHF, i.e., the energy is minimum only when $\nu_1 = \nu_3 = 1/2$.

We solve the two-particle Green's function,

$$\chi^{\sigma,\sigma'}_{\gamma,\gamma'}(\mathbf{q},\mathbf{q}';\tau-\tau') = -N_\phi\langle T\delta\rho_{\sigma,\sigma'}(\mathbf{q},\tau)\delta\rho_{\gamma,\gamma'}(-\mathbf{q}',\tau')\rangle,$$

with the time order operator T and $\delta\rho = \rho - \langle\rho\rangle$, in the generalized random-phase approximation (GRPA) [20,21] to study the collective behavior of the system. The lowest-energy collective mode given by the poles of the retarded Green's functions is

$$C(\mathbf{q} = \mathbf{0}) = \frac{e^2}{\kappa\ell}|Q(\nu_1 - \nu_3)|, \tag{13}$$

where $C(\mathbf{q})$ is the dispersion relation between the collective and the momentum. This mode, which is similar to that of an easy-plane QHF in a double-quantum-well system without tunneling, is a precess mode of the valley pseudospin in the xy plane [20,22]. In the three types of QHFs, when $\mathbf{q} \to \mathbf{0}$, the collective modes are distinguished by their gaps and the behaviors at small q. In a SU(2) QHF, $Q = 0$, so $C(\mathbf{0}) = 0$. It is a goldstone mode. In an easy-plane QHF, $\nu_1 - \nu_3 = 0$, so $C(\mathbf{0}) = 0$, which means a goldstone mode still exists. In these

two QHFs, $C(\mathbf{q}\to\mathbf{0})\propto q$. In an Ising QHF, $C(\mathbf{q}\to\mathbf{0})\propto q^2$, $Q\neq 0$, and $|\nu_1-\nu_3|=1$. The goldstone mode disappears and all modes are gapped.

IV. MANY-BODY HAMILTONIAN OF SILICENE/GERMANENE IN THE PRESENCE OF A MAGNETIC FIELD

The Hamiltonian in Eq. (1) is more complex than that in Eq. (2) since the electric field and the RSO coupling are included. In the QH, the wave function in valley α and orbital o is

$$\psi_o^\alpha=\left(c_{o,1}^\alpha h_{o+\alpha_1}\ c_{o,2}^\alpha h_{o+\alpha_2}\ c_{o,3}^\alpha h_{o+\alpha_3}\ c_{o,4}^\alpha h_{o+\alpha_4}\right)^T, \tag{14}$$

with the normalization condition $\sum_{i=1}^4|c_{o,i}^\alpha|^2=1$, where $\alpha_i=K_i,K_i'$ shortens the indices of the wave-function spinors in valley α and corresponds to $K_1=K_4=0,K_2=-1,K_3=1;K_1'=-1,K_2'=K_3'=0,K_4'=1$. Because of the RSO coupling, the eigenvectors are not spin-polarized. We introduce another degree of freedom, the orbital, to replace the spin. We find that without Zeeman coupling, the energies of the orbitals $o=N,N-1$ are close to each other in the LL N. The concept of the orbital degree of freedom here is similar to that in the $N=0$ LL in bilayer graphene. The RSO interaction couples different spins in a valley. For zero RSO coupling, the orbital degree of freedom is identical to spin. In reality, $|c_{N-1,1}^\alpha|,|c_{N-1,2}^\alpha|,|c_{N,3}^\alpha|,|c_{N,4}^\alpha|\lesssim 10^{-4}$, and so approximately the orbital N is associated with spin up and the orbital $N-1$ is associated with spin down. Note that the coefficients $c_{o,i}^\alpha$ depend not only on the magnetic field but also on the electric field.

We neglect the LL mixing since the LL gap is large ($E_{N=0}\sim 0,E_{N=1}\approx 60$ meV for silicene). The elements of the density matrix with an extra orbital index can be obtained by modifying Eq. (4):

$$\rho_{\alpha,o;\beta,o'}(\mathbf{q})=\frac{1}{N_\phi}\sum_{X_1,X_2}e^{-\frac{i}{2}q_x(X_1+X_2)}\delta_{X_1,X_2+q_y\ell^2}\times c_{\alpha,o,X_1}^\dagger c_{\beta,o',X_2}, \tag{15}$$

where α,β are valley indices and o,o' are orbital indices. There is not conservation between orbitals, so the many-body Hamiltonian in the HFA is more complex than that in Eq. (5),

$$\begin{aligned}H=&\frac{e^2}{\kappa\ell}\sum_{\alpha,o}\widetilde{E}_{\alpha,o}\rho_{\alpha,o;\alpha,o}(0)\\&+\frac{e^2}{\kappa\ell}\sum_{\alpha,\beta}\sum_{o_1,\ldots,o_4}\overline{\sum_{\mathbf{q}}}H_{o_1,o_2,o_3,o_4}^{\alpha,\beta}(\mathbf{q})\\&\times\langle\rho_{\alpha,o_1;\alpha,o_2}(-\mathbf{q})\rangle\rho_{\beta,o_3;\beta,o_4}(\mathbf{q})\\&-\frac{e^2}{\kappa\ell}\sum_{\alpha,\beta}\sum_{o_1,\ldots,o_4}\sum_{\mathbf{q}}X_{o_1,o_4,o_3,o_2}^{\alpha,\beta}(\mathbf{q})\\&\times\langle\rho_{\alpha,o_1;\beta,o_2}(-\mathbf{q})\rangle\rho_{\beta,o_3;\alpha,o_4}(\mathbf{q}),\end{aligned} \tag{16}$$

where $\widetilde{E}_{\alpha,o}$ contains the kinetic energy $E_{\alpha,o}$ of the orbital o in valley α and a capacitive energy,

$$\widetilde{E}_{\alpha,o}=E_{\alpha,o}+\frac{d}{\ell}\left[\frac{\nu}{2}-\sum_{\beta,o'}U_{\alpha,o;\beta,o'}^0\langle\rho_{\beta,o';\beta,o'}(0)\rangle\right],$$

$$U_{\alpha,o;\beta,o'}^0=\left(\sum_{i=1,3}\sum_{j=2,4}+\sum_{i=2,4}\sum_{j=1,3}\right)|c_{o,i}^\alpha|^2|c_{o',j}^\beta|^2,$$

with the filling factor ν. The Hartree interaction is

$$\begin{aligned}H_{o_1,o_2,o_3,o_4}^{\alpha,\beta}(\mathbf{q})=&\sum_{m,n=1}^{2}\sum_{i=m,m+2}\sum_{j=n,n+2}G_{1,2,3,4}^{\alpha,\beta;i,j}\\&\times P_{m,n}(q\ell)\frac{F_{1,2,3,4}}{q\ell}\Theta_{o_1+\alpha_i,o_2+\alpha_i}(q\ell)\Theta_{o_3+\beta_j,o_4+\beta_j}(q\ell),\end{aligned} \tag{17}$$

where we define a function $P_{m,n}(q)=e^{-|m-n|qd/\ell-q^2/2}$ and coefficients

$$G_{1,2,3,4}^{\alpha,\beta;i,j}=c_{o_1,i}^{\alpha*}c_{o_2,i}^{\alpha}c_{o_3,j}^{\beta*}c_{o_4,j}^{\beta}, \tag{18}$$

$$F_{1,2,3,4}=e^{-i(o_1-o_2)\theta}e^{-i(o_3-o_4)(\theta+\pi)}, \tag{19}$$

with the angle θ between vector $\mathbf{q}$ and the x axis. Function Θ is defined by

$$\Theta_{k,l}(p)=\frac{\sqrt{\min(k,l)!}}{\sqrt{\max(k,l)!}}\frac{(ip)^{|k-l|}}{\sqrt{2}^{|k-l|}}L_{\min(k,l)}^{|k-l|}\left(\frac{p^2}{2}\right). \tag{20}$$

The Fock interaction is

$$\begin{aligned}X_{o_1,o_4,o_3,o_2}^{\alpha,\beta}(\mathbf{q})=&\sum_{m,n=1}^{2}\sum_{i=m,m+2}\sum_{j=n,n+2}G_{1,4,3,2}^{\alpha,\beta;i,j}e^{-(o_1-o_4+o_3-o_2)i\theta}\\&\times\int dp\ P_{m,n}(p)J_{o_1-o_4+o_3-o_2}(pq\ell)\\&\times\Theta_{o_1+\alpha_i,o_4+\alpha_i}(p)\Theta_{o_3+\beta_j,o_2+\beta_j}(-p).\end{aligned} \tag{21}$$

We define the Green's function

$$G_{\alpha,o;\beta,o'}(X,X',\tau)=-\langle Tc_{\alpha,o,X}(\tau)c_{\beta,o',X'}^\dagger(0)\rangle, \tag{22}$$

with a relation to the density matrix at zero temperature, $G_{\alpha,o;\beta,o'}(\mathbf{q},\tau=0^-)=\langle\rho_{\beta,o';\alpha,o}(\mathbf{q})\rangle$. Solving the equation of motion of the Green's function, we could obtain the ground states of the system [23]. In what follows, we define the valley-orbital (or, say, valley-spin if $\lambda_R=0$) indices as $(K,N)\to 1,(K,N-1)\to 2,(K',N)\to 3,(K',N-1)\to 4$ in the density matrix. The orbital degree of freedom replaces the spin, so the two-particle Green's function based on the density matrix in Eq. (15) should be written as

$$\begin{aligned}\chi_{\eta_3,o_3;\eta_4,o_4}^{\eta_1,o_1;\eta_2,o_2}(\mathbf{q},\mathbf{q}';\tau-\tau')=&-N_\phi\langle T\delta\rho_{\eta_1,o_1;\eta_2,o_2}(\mathbf{q},\tau)\\&\times\delta\rho_{\eta_3,o_3;\eta_4,o_4}(-\mathbf{q}',\tau')\rangle,\end{aligned} \tag{23}$$

where $\eta_i=K,K'$ is the valley index.

Due to the electron-hole symmetry, we consider only the quarter- and half-filled LLs. The system can be described in the (pseudo)spin language. The valley pseudospin field in orbital

o is defined by

$$p_{o,x} + ip_{o,y} = \langle \rho_{K,o;K',o} \rangle, \tag{24}$$

$$p_{o,z} = \langle \rho_{K,o;K,o} \rangle - \langle \rho_{K',o;K',o} \rangle, \tag{25}$$

$$\mathbf{p} = \sum_o \mathbf{p}_o. \tag{26}$$

We could approximately associate the orbital with the real spin: $o = N$ associated with spin up and $o = N-1$ associated with spin down. Hence, we define the spin field

$$S_{\alpha,x} + iS_{\alpha,y} = \langle \rho_{\alpha,N;\alpha,N-1} \rangle, \tag{27}$$

$$S_{\alpha,z} = \langle \rho_{\alpha,N;\alpha,N} \rangle - \langle \rho_{\alpha,N-1;\alpha,N-1} \rangle, \tag{28}$$

$$\mathbf{S} = \sum_\alpha \mathbf{S}_\alpha. \tag{29}$$

V. NUMERICAL RESULTS OF LLs $N = 0,1$

Filling factor $\nu = -1$: When $E_z = 0$, the ground state is an easy-plane QHF in valley pseudospin with $\langle \rho_{1,1}(\mathbf{0}) \rangle = \langle \rho_{3,3}(\mathbf{0}) \rangle = 1/2$, which is essentially equivalent to that in a double-quantum-well system [24]. It can also be obtained by the classification parameter Q in Eq. (12): If we approximate $\lambda_R = 0$, then $Q > 0$, i.e., easy-plane QHF. When the electric field increases, there is a bias between the two states $|1\rangle$ and $|3\rangle$ so that the ground state is a bonding state $|\mathrm{GS}\rangle = a_1|1\rangle + a_3|3\rangle$. When the electric field $E_z \gtrsim 0.08$ mV/nm, the bias is large enough to polarize the valley. The coherence between $|1\rangle$ and $|3\rangle$ also vanishes gradually. The order parameters in the phase transition are shown in Fig. 1(a).

For an easy-plane QHF, the charged excitation is a bimeron or an antibimeron described in the anisotropic nonlinear σ model [25]. At $E_z = 0$, we extract the Fock energy functional from the Hamiltonian

$$H_F = -\frac{e^2}{\kappa \ell} \sum_{\alpha,\beta} \sum_{o_1,o_2,o_3,o_4} \sum_{\mathbf{q}} X^{\alpha,\beta}_{o_1,o_4,o_3,o_2}(\mathbf{q}) \times \langle \rho_{\alpha,o_1;\beta,o_2}(-\mathbf{q}) \rangle \rho_{\beta,o_3;\alpha,o_4}(\mathbf{q}), \tag{30}$$

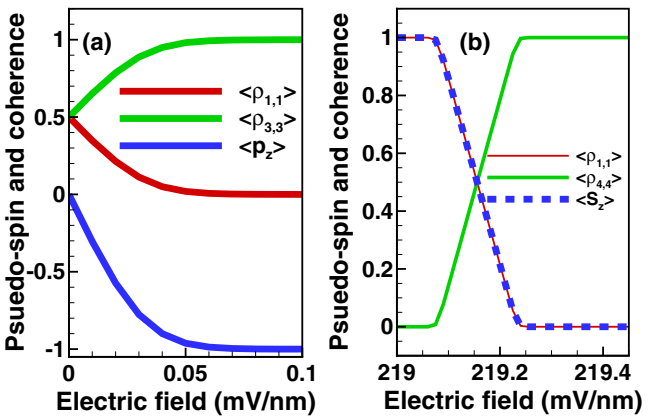

FIG. 1. (Color online) (a) The occupation of the states $|1\rangle$ and $|3\rangle$, and the valley polarization $\langle p_z \rangle$ at $\nu = -1$. (b) Order parameters around the phase-transition region at $\nu = 0$. The dielectric constant κ is 1.

where we neglect the kinetic energy, capacitive energy, and Hartree interaction. This is because the kinetic energy is a constant, capacitive energy is very small, and the Hartree term is zero in the slow varied density approximation. This field theory is only valid when $E_z = 0$. If $E_z \neq 0$, then the ground state is no longer an easy-plane QHF. The ground state will be valley-polarized very rapidly, i.e., the E_z is very small to polarize the valley pseudospin. In the finite E_z case, the best way is to calculate the microscopic Hamiltonian in the symmetric gauge [10,26].

If we consider the two valleys only in orbital $o = N$, then the orbital index could be neglected. The energy is given by

$$E_F = -\frac{1}{2}\frac{e^2}{\kappa \ell} \sum_{\alpha,\beta} \sum_{\mathbf{q}} X^{\alpha,\beta}_{N,N,N,N}(\mathbf{q}) \times \langle \rho_{\alpha,\beta}(-\mathbf{q}) \rangle \langle \rho_{\beta,\alpha}(\mathbf{q}) \rangle. \tag{31}$$

Then the Lagrangian of the anisotropic nonlinear σ model is obtained by calculating the excitation energy when the density matrix is slowly varied [25],

$$L = \frac{1}{2} \sum_{\mu=x,y,z} \rho_\mu (\partial_\mu m_\mu)^2, \tag{32}$$

where the normalized pseudospin field $\mathbf{m}$ is defined in real space by

$$m_x(\mathbf{r}) + im_y(\mathbf{r}) = 4\pi \ell^2 \langle \rho_{K,K'}(\mathbf{r}) \rangle, \tag{33}$$

$$m_z(\mathbf{r}) = 4\pi \ell^2 [\langle \rho_{K,K}(\mathbf{r}) \rangle - \langle \rho_{K',K'}(\mathbf{r}) \rangle], \tag{34}$$

and the pseudospin stiffnesses are given by

$$\rho_z = -\frac{1}{8\pi \ell^2} \lim_{q \to 0} \nabla_q^2 X^{K,K}_{N,N,N,N}(\mathbf{q}), \tag{35}$$

$$\rho_x = \rho_y = -\frac{1}{8\pi \ell^2} \lim_{q \to 0} \nabla_q^2 X^{K,K'}_{N,N,N,N}(\mathbf{q}). \tag{36}$$

The excitation energy of a bimeron or an antibimeron is

$$\delta E = \frac{4\pi}{3}(\rho_x + \rho_y + \rho_z). \tag{37}$$

Note that this energy that is obtained in the field theory is not identical to a single charged excitation of the electron gas. But the excitation energy of a bimeron-antibimeron pair in the field theory is identical to that in the electron gas, which is double δE, $\delta E_{\mathrm{pair}} = 2\delta E$. This energy is related to the transport property of the system, which can be measured in a transport experiment. For $B = 10$ T and $\kappa = 1$, the excitation energy of a bimeron-antibimeron pair is 39.2 meV. In comparison, the excitation energy of an electron-hole pair is 156 meV. Hence, the transport gap is due to the bimeron-antibimeron pair.

Filling factor $\nu = 0$: When $E_z < 219.05$ mV/nm, $|1\rangle$ and $|3\rangle$ are fully occupied, the ground state is spin-polarized and is valley-unpolarized. In the region $E_z \in [219.05, 219.25]$ mV/nm, the coherence $\langle \rho_{1,4} \rangle$ between $|1\rangle$ and $|4\rangle$ arises. When $E_z > 219.25$ mV/nm, the system is spin-unpolarized but valley-polarized, and all electrons are in valley K'. The phase transition, where $\langle \rho_{1,1} \rangle$ and $\langle \rho_{4,4} \rangle$ are gradually changed, is shown in Fig. 1(b). The spin and the valley are also controlled gradually by the electric field.

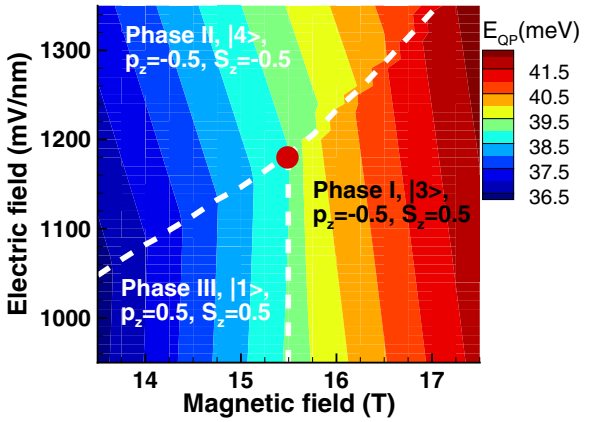

FIG. 2. (Color online) The excitation energy contour of the quasiparticle around the triple point at $\nu = 3, \kappa = 5$. The dashed lines are located at the phase transitions. The red dot is the triple point.

In the $N > 0$ LLs, the nature of the broken symmetry states is different from that in LL $N = 0$. For $N > 0$, the ground state at integer filling factor is an Ising QHF, which is similar to bilayer graphene [9,10]. We only study the filling factors $\nu = 3,4$, since the LL mixing is important in higher LLs.

Filling factor $\nu = 3$: For $E_z = 0$, we assume $\lambda_R = 0$ to obtain $Q < 0$. Hence the ground state is an Ising QHF, which is also supported by our numerical calculation including λ_R. The SU(2) valley symmetry is broken to a Z_2 symmetry. Figure 2 shows the phase diagram in an electric field for $\kappa = 5$. The SU(2) spin symmetry is also broken to a Z_2 symmetry at the phase transition between phase I (III) and phase II. These symmetry broken states are all induced by the small buckling. The valley and spin can also be controlled by the electric or the magnetic field, since the valley or spin is reversed at the two sides of the phase transition line in Fig. 2.

Interestingly, for $B = 15.5$ T and $E_z = 1180$ mV/nm, there is a triple point (the red dot in Fig. 2) in the phase diagram. This triple point occurs only when $\kappa \gtrsim 3$. When the dielectric constant is very large, the electron gas is close to a noninteracting system and the triple point disappears. The phase diagram is also changed by the dielectric constant κ.

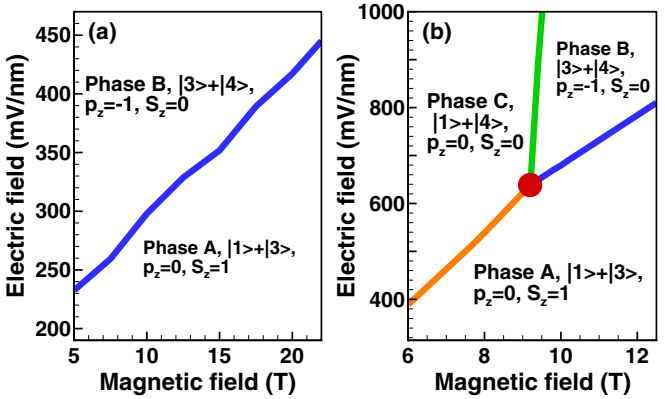

FIG. 3. (Color online) The phase diagrams at $\nu = 4$ and (a) $\kappa = 1$, (b) $\kappa = 4$.

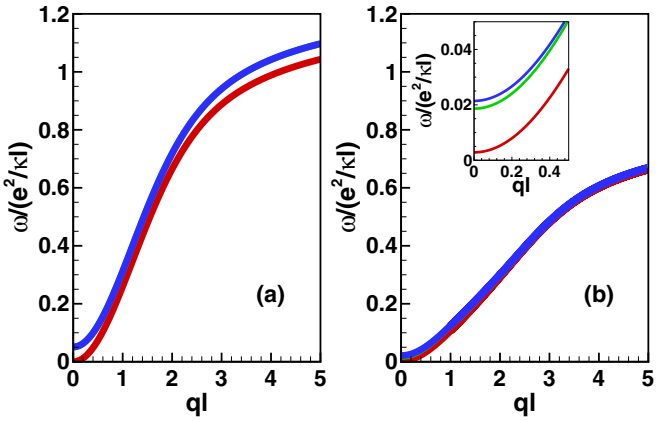

FIG. 4. (Color online) The collective modes for (a) the easy-plane QHF ground state at $\nu = -1$ and (b) the Ising QHF ground state at $\nu = 3$, when $B = 10$ T, $\kappa = 1$, and $E_z = 0$. The small-q region is given as an inset.

For $\kappa = 1$, the phase III disappears and only other two phases survive when $E_z < 2000$ mV/nm.

The Ising QHF here is similar to that in bilayer or multilayer graphene [10], but it is different from the Ising QHF with different LLs [27] in semiconductor quantum wells. Hence, the lowest charged excitation may be a skyrmion around $E_z = 0$. However, the skyrmion must be calculated numerically with a microscopic Hamiltonian in the symmetric gauge.

There is no domain wall at zero temperature. At finite temperature, the domain wall could exist to lower the free energy of the system [28] when we consider the wall entropy. Below a critical temperature T_C, domain walls provide one-dimensional (1D) channels carrying extra charges (electron-hole pairs) to dissipate the transport charge of the 2DEG when the domain walls are dense enough to overlap. So the resistance spike in R_{xx} appears. Above T_C, the domain wall will be infinitely long and expand to the sample perimeter. The charge in the domain wall cannot dissipate the transport electrons

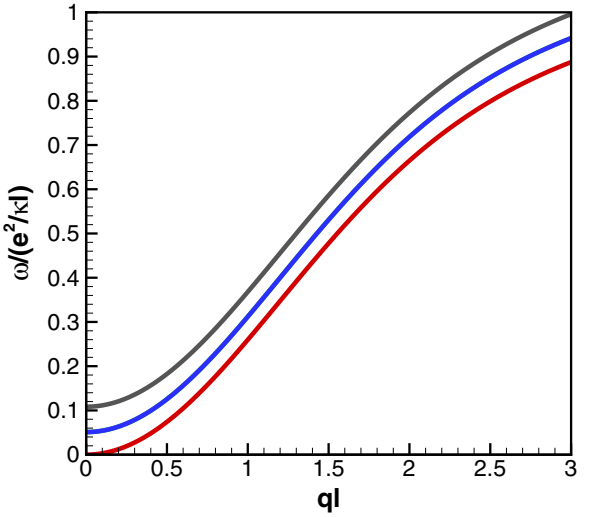

FIG. 5. (Color online) The dispersion of the collective modes for $B = 10$ T, $\kappa = 1$, and $E_z = 219.15$ mV/nm at $\nu = 0$.

anymore and hence the resistance spike disappears. Following the study of the domain wall in a graphene bilayer [10], we obtain the kink domain wall of the valley pseudospin at $E_z = 0$: $m_x(\mathbf{r}) = \sin\theta(\mathbf{r})$, $m_y = 0$, and $m_z(\mathbf{r}) = \cos\theta(\mathbf{r})$ with

$$\theta = 2\arctan\exp\left[\sqrt{2\frac{K_z - K_\perp}{\rho_s}}x\right], \tag{38}$$

where we approximate $\rho_s = \rho_x \approx \rho_z$, and we define $K_\perp = X^{K,K'}_{N,N,N,N}(\mathbf{0})/(8\pi)$ and $K_z = X^{K,K}_{N,N,N,N}(\mathbf{0})/(8\pi)$. It should be noted that some other edge states that are important, especially in the $N = 0$ LL of monolayer and bilayer graphene [29], may change the transport properties to a certain extent.

We also present the quasiparticle (QP) energy $E_{\rm QP}$ around the triple point in Fig. 2. Experimentally, the phase transitions between different spins can be observed in a NMR experiment. The phase transition between different valleys may be observed in a circular light absorption experiment [30]. At the phase transitions, a resistivity spike may be observed in a transport experiment due to the existence of the domain walls at finite temperature, which has been reported in a LL Ising QHF [27,28] and in the Ising QHF of bilayer graphene [10,11].

Filling factor $\nu = 4$: For $\kappa = 1$, the phase diagram in a magnetic field is shown in Fig. 3(a). The triple point also appears when $\kappa \gtrsim 3$. It is marked as a red dot located at $B = 9.2$ T and $E_z = 635$ mV/nm for $\kappa = 4$ in Fig. 3(b). Phase C sets in when $B < 9.2$ T, since the kinetic energy contributes more and the Coulomb interaction is decreased by large κ.

As we discussed above, the easy-plane QHFs have a goldstone mode while all the modes of Ising QHFs are gapped. In silicene, we are also able to find the goldstone and the gapped modes for the easy-plane QHF and Ising QHF ($\nu = -1$ and 3, respectively) in Fig. 4. Moreover, in the region $E_z \in [219.05, 219.25]$ mV/nm, the ground state is a bonding state with a goldstone mode at $\nu = 0$. The dispersion of the collective modes is shown in Fig. 5.

VI. CONCLUSION

We classify the ground states of a generic buckled Dirac material in a magnetic field into three different QHFs. The low-energy collective modes of the three QHFs are given analytically in the GRPA. A goldstone mode exists in the SU(2) and the easy-plane QHFs, but not in the Ising QHF. We then focus on a real material, viz., silicene. Without an electric field we note that the magnetic field is able to change the coefficients $c^{\alpha}_{o,i}$ in the wave functions. However, in a very small magnetic field ($B \ll 0.01$ T), the ground state becomes an easy-plane QHF at $\nu = 3$. In such a low magnetic field, the QH effect cannot be realized and the LL mixing is not negligible. If the SO coupling can be tuned, then the coefficients of wave functions can be modified. For $B = 10$ T, $\nu = 3$, and $\kappa = 1$, we find that when $\lambda_{\rm SO} > 750$ meV, the ground state is an easy-plane QHF. For $\lambda_{\rm SO} \approx 750$ meV, the ground state is a SU(2) QHF. If we could efficiently tune the wave function, we may realize the phase transition between different QHFs (also in germanene). Experimentally, this transition is observable: the domain wall induced resistivity spike occurs only in an Ising QHF. The phase diagrams and transport properties in the $N = 0,1$ LLs in silicene depend on the magnetic field and the dielectric constant, which dramatically change the Coulomb interaction. At $\nu = 0$, the intervalley scattering or lattice-scale interactions make the ground state inhomogeneous with various orders in graphene [31]. In silicene/germanene systems, this interactions may also change the QHF ground state to other ordered states at $\nu = 0$, which needs to be verified experimentally. We show the triple points in Figs. 2 and 3. The SU(2) symmetry of the spin and valley are broken by the electric field and the buckling structure. The phase transitions may indeed be observed in NMR, transport, or light absorption experiments.

ACKNOWLEDGMENT

The work has been supported by the Canada Research Chairs Program of the Government of Canada.

[1] K. Takeda and K. Shiraishi, Phys. Rev. B **50**, 14916 (1994); C.-C. Liu, W. Feng, and Y. Yao, Phys. Rev. Lett. **107**, 076802 (2011); Y. Wang, J. Zheng, Z. Ni, R. Fei, Q. Liu, R. Quhe, C. Xu, J. Zhou, Z. Gao, and J. Lu, Nano **07**, 1250037 (2012); F.-B. Zheng and C.-W. Zhang, Nanoscale Res. Lett. **7**, 422 (2010); A. Kara, H. Enriquez, A. P. Seitsonen, L. C. Lew, Yan Voon, S. Vizzini, B. Aufray, and H. Oughaddou, Surf. Sci. Rep. **67**, 1 (2012); Q. Tang and Z. Zhou, Progr. Mater. Sci. **58**, 1244 (2013); H. Rostami, A. G. Moghaddam, and R. Asgari, Phys. Rev. B **88**, 085440 (2013); A. Kormanyos, V. Zolyomi, N. D. Drummond, P. Rakyta, G. Burkard, and V. I. Falko, *ibid.* **88**, 045416 (2013).

[2] Q. H. Wang, K. Kalantar-Zadeh, A. Kis, J. N. Coleman, and M. S. Strano, Nat. Nanotech. **7**, 699 (2012).

[3] *Physics of Graphene*, edited by H. Aoki and M. S. Dresselhaus (Springer, New York, 2014).

[4] D. S. L. Abergel, V. Apalkov, J. Berashevich, K. Ziegler, and T. Chakraborty, Adv. Phys. **59**, 261 (2010).

[5] T. Chakraborty and V. Apalkov, in Ref. [3], Chap. 8; T. Chakraborty and V. M. Apalkov, Solid State Commun. **175**, 123 (2013); T. Chakraborty and P. Pietiläinen, Phys. Rev. Lett. **76**, 4018 (1996); D. S. L. Abergel and T. Chakraborty, *ibid.* **102**, 056807 (2009); V. M. Apalkov and T. Chakraborty, *ibid.* **97**, 126801 (2006); **105**, 036801 (2010); **107**, 186803 (2011).

[6] V. M. Apalkov and T. Chakraborty, Phys. Rev. B **90**, 245108 (2014).

[7] V. M. Apalkov and T. Chakraborty, Phys. Rev. B **91**, 235447 (2015).

[8] Z. Y. Zhu, Y. C. Cheng, and U. Schwingenschlögl, Phys. Rev. B **84**, 153402 (2011); G.-B. Liu, W.-Y. Shan, Y. Yao, W. Yao, and D. Xiao, *ibid.* **88**, 085433 (2013); J. E. Padilha, H. Peelaers, A. Janotti, and C. G. Van de Walle, *ibid.* **90**, 205420 (2014); Y.-H. Ho, W.-P. Su, and M.-F. Lin, RSC Adv. **5**, 20858 (2015).

[9] W. Luo, R. Côté, and A. Bédard-Vallée, Phys. Rev. B **90**, 075425 (2014).

[10] W. Luo and R. Côté, Phys. Rev. B **90**, 245410 (2014).

[11] K. Lee, B. Fallahazad, J. Xue, D. C. Dillen, K. Kim, T. Taniguchi, K. Watanabe, and E. Tutuc, Science **345**, 58 (2014).
[12] M. Tahir and U. Schwingenschlögl, Sci. Rep. **3**, 1075 (2013).
[13] Z. Ni, Q. Liu, K. Tang, J. Zheng, J. Zhou, R. Qin, Z. Gao, D. Yu, and J. Lu, Nano Lett. **12**, 113 (2012); M. Ezawa, New J. Phys. **14**, 033003 (2012); J. Phys. Soc. Jpn. **81**, 064705 (2012).
[14] C.-C. Liu, H. Jiang, and Y. Yao, Phys. Rev. B **84**, 195430 (2011).
[15] N. J. Roome and J. D. Carey, ACS Appl. Mater. Interf. **6**, 7743 (2014).
[16] F. D. M. Haldane, Phys. Rev. Lett. **61**, 2015 (1988).
[17] Y.-X. Wang, F.-X. Li, and Y.-M. Wu, Europhys. Lett. **105**, 17002 (2014).
[18] C. L. Kane and E. J. Mele, Phys. Rev. Lett. **95**, 226801 (2005).
[19] E. I. Rashba, Phys. Rev. B **79**, 161409(R) (2009).
[20] R. Côté, D. B. Boisvert, J. Bourassa, M. Boissonneault, and H. A. Fertig, Phys. Rev. B **76**, 125320 (2007).
[21] J. Lambert and R. Côté, Phys. Rev. B **87**, 115415 (2013).
[22] Z. F. Ezawa, Phys. Rev. Lett. **82**, 3512 (1999); Z. F. Ezawa and A. Sawada, Physica B **294-295**, 463 (2001); Z. F. Ezawa and G. Tsitsishvili, Phys. Rev. B **70**, 125304 (2004).
[23] R. Côté and A. H. MacDonald, Phys. Rev. Lett. **65**, 2662 (1990); Phys. Rev. B **44**, 8759 (1991).
[24] J. P. Eisenstein and A. H. MacDonald, Nature (London) **432**, 691 (2004); J. P. Eisenstein, Annu. Rev. Condens. Matter Phys. **5**, 159 (2014).
[25] K. Moon, H. Mori, K. Yang, S. M. Girvin, A. H. MacDonald, L. Zheng, D. Yoshioka, and S.-C. Zhang, Phys. Rev. B **51**, 5138 (1995).
[26] H. A. Fertig, L. Brey, R. Côté and A. H. MacDonald, Phys. Rev. B **50**, 11018 (1994); W. Luo and R. Côté, *ibid.* **88**, 115417 (2013).
[27] A. J. Daneshvar, C. J. B. Ford, M. Y. Simmons, A. V. Khaetskii, A. R. Hamilton, M. Pepper, and D. A. Ritchie, Phys. Rev. Lett. **79**, 4449 (1997); T. Jungwirth, S. P. Shukla, L. Smrčka, M. Shayegan, and A. H. MacDonald, *ibid.* **81**, 2328 (1998); V. Piazza, V. Pellegrini, F. Beltram, W. Wegscheider, T. Jungwirth, and A. H. MacDonald, Nature (London) **402**, 638 (1999).
[28] T. Jungwirth and A. H. MacDonald, Phys. Rev. Lett. **87**, 216801 (2001); Phys. Rev. B **63**, 035305 (2000).
[29] H. A. Fertig and L. Brey, Phys. Rev. Lett. **97**, 116805 (2006); M. Killi, T.-C. Wei, I. Affleck, and A. Paramekanti, *ibid.* **104**, 216406 (2010); G. Murthy, E. Shimshoni, and H. A. Fertig, Phys. Rev. B **90**, 241410 (2014); K. Dhochak, E. Shimshoni, and E. Berg, *ibid.* **91**, 165107 (2015).
[30] C. J. Tabert and E. J. Nicol, Phys. Rev. Lett. **110**, 197402 (2013).
[31] J. Jung and A. H. MacDonald, Phys. Rev. B **80**, 235417 (2009); R. Nandkishore and L. S. Levitov, Phys. Scr. **T146**, 014011 (2012); M. Kharitonov, Phys. Rev. Lett. **109**, 046803 (2012); Phys. Rev. B **85**, 155439 (2012); A. F. Young, J. D. Sanchez-Yamagishi, B. Hunt, S. H. Choi, K. Watanabe, T. Taniguchi, R. C. Ashoori, and P. Jarillo-Herrero, Nature (London) **505**, 528 (2014); F. Wu, I. Sodemann, Y. Araki, A. H. MacDonald, and T. Jolicoeur, Phys. Rev. B **90**, 235432 (2014).